mTORC1 controls lysosomal Ca2+ release through the two-pore channel TPC2

One-sentence summary: The ion channel TPC2 is required for Ca^{2+} mobilization from lysosomes in response to mTORC1 inhibition and to NAADP.

Editor's summary:
Channeling lysosomal Ca^{2+}
Autophagy, or the digestion of macromolecules and organelles by lysosomes, is regulated by the multiprotein complex mTORC1. TPC2 is a lysosomal channel that carries Ca^{2+} or Na^{+} flux in response to different ligands and promotes the termination of autophagy. Using mouse pulmonary arterial myocytes and cells expressing TPC2, Ogunbayo *et al.* identified mTORC1 inhibition as a mechanism for TPC2 activation that led to the mobilization of Ca^{2+} from lysosomes. Furthermore, they showed that TPC2 may be regulated by mTORC1 inhibition and NAADP through a common pathway. Autophagy is increased in pulmonary hypertension, and the authors suggest that modulating TPC2 activity could be a promising therapeutic strategy for this condition, which currently lacks effective treatments.

mTORC1 controls lysosomal Ca^{2+} release through the two-pore channel TPC2

[1]Oluseye A. Ogunbayo, [1]Jingxian Duan, [2]Jian Xiong, [2]Qiaochu Wang, [2]Xinghua Feng, [3]Jianjie Ma, [2]Michael X. Zhu, [1]A. Mark Evans

[1]Centres for Discovery Brain Sciences and Cardiovascular Sciences, Edinburgh Medical School: Biomedical Sciences, University of Edinburgh, Edinburgh, EH8 9XD, Scotland UK.

[2]Department of Integrative Biology and Pharmacology, McGovern Medical School, Program in Biochemistry and Cell Biology, Graduate School of Biomedical Sciences, The University of Texas Health Science Center at Houston, Houston, TX 77030, USA.

[3]Department of Surgery, Davis Heart and Lung Research Institute, The Ohio State University, Columbus, OH 43210, USA.

Corresponding Author: A. Mark Evans, [1]Centres for Discovery Brain Sciences and Cardiovascular Sciences, Edinburgh Medical School: Biomedical Sciences, University of Edinburgh, Hugh Robson Building, George Square, Edinburgh EH8 9XD, UK

Fax: +44 (0) 131 650 6527; Telephone: +44 (0) 131 651 1501; Email: mark.evans@ed.ac.uk

Abstract

Two-pore segment channel 2 (TPC2) is a ubiquitously expressed, lysosomally targeted ion channel that aids

in terminating autophagy and is inhibited upon its association with mechanistic target of rapamycin (mTOR). It is controversial whether TPC2 mediates lysosomal Ca^{2+} release or selectively conducts Na^{+}, and whether the binding of nicotinic acid adenine dinucleotide phosphate (NAADP) or phosphatidylinositol 3,5-bisphosphate ($PI(3,5)P_2$) is required for the activity of this ion channel. Here we show that TPC2 is required for intracellular Ca^{2+} signaling in response to NAADP or to mTOR inhibition by rapamycin. In pulmonary arterial myocytes, rapamycin and NAADP evoked global Ca^{2+} transients that were blocked by depletion of lysosomal Ca^{2+} stores. Pre-incubation of cells with high concentrations of rapamycin resulted in desensitization and blocked NAADP-evoked Ca^{2+} signals. Moreover, rapamycin and NAADP did not evoke discernable Ca^{2+} transients in myocytes derived from *Tpcn2* knockout mice, which showed normal responses to other Ca^{2+}-mobilizing signals. In HEK293 cells stably overexpressing human TPC2, shRNA-mediated knockdown of mTOR blocked rapamycin- and NAADP-evoked Ca^{2+} signals. Confocal imaging of a genetically encoded Ca^{2+} indicator fused to TPC2 demonstrated that rapamycin-evoked Ca^{2+} signals localized to lysosomes and were in close proximity to TPC2. Therefore, inactivation of mTOR may activate TPC2 and consequently lysosomal Ca^{2+} release.

INTRODUCTION

The two-pore segment channels (TPCs) (*1*) are NAADP-gated Ca^{2+} release channels that are targeted to endolysosomes (*2-7*). Consistent with this view TPC1, TPC2 and TPC3, of which only *TPCN1* and *TPCN2* genes (*2, 8*) are present in humans, rats and mice, are homologous with and represent an evolutionary intermediate between some Ca^{2+}-permeable transient receptor potential (TRP) channels and voltage-gated Ca^{2+} channels (CaV), with an intermediate two-domain structure of subunits which likely assemble as homodimers (*2, 8*). However, controversy surrounds the capacity of TPC2 to support an NAADP-gated Ca^{2+} conductance, given that others have demonstrated that human TPC2 expressed in several different mammalian cell types is highly selective for Na^+ and carries a Na^+ conductance in response to phosphatidylinositol 3,5-bisphosphate ($PI(3,5)P_2$) but not NAADP (*7, 9, 10*). Countering this notion, cells derived from *Tpcn1* and *Tpcn2* null mice generate $PI(3,5)P_2$-mediated cation currents but not NAADP-gated Ca^{2+} currents, and NAADP-dependent cation currents are restored in *Tpcn1* and *Tpcn2* null cells by overexpression of wild type TPC2 (*11*). That said, it is clear that TPC2 mediates a Na^+ conductance that is gated by inhibition of mechanistic Target of Rapamycin (mTOR) (*10*) and TPC2 contributes to autophagy termination and mTOR reactivation (*12*). Activation of mTORC1 has been implicated in the progression of diseases such as pulmonary hypertension for which current therapies are ineffective (*13*). Therefore, we sought to determine whether TPC2 mediates lysosomal Ca^{2+} signals in pulmonary arterial myocytes upon intracellular dialysis of NAADP and $PI(3,5)P_2$, respectively, and the role of mTOR in these processes.

RESULTS

TPC2 deletion in pulmonary arterial myocytes abolishes global Ca^{2+} waves in response to NAADP but not $PI(3,5)P_2$, $I(1,4,5)P_3$ or cADPR

We examined the action of various Ca^{2+} mobilising messengers in pulmonary arterial myocytes prepared from wild type mice and *Tpcn2* knockout mice (*2, 12*), by employing intracellular dialysis from a patch pipette under voltage-clamp, with the holding potential set to -40 mV to inactivate voltage-gated Ca^{2+} channels. Intracellular dialysis of NAADP induced global Ca^{2+} waves in acutely isolated pulmonary arterial myocytes from wild type mice (Fig. 1A). By contrast NAADP did not induce a measurable Ca^{2+} transient in paired experiments on myocytes derived from *Tpcn2* knockout mice (Fig. 1A), as assessed by the Fura-2 F340 / F380 ratio. In contrast, the response to intracellular dialysis of either $PI(3,5)P_2$, $I(1,4,5)P_3$ or cADPR

was similar in myocytes derived from *Tpcn2* knockout mice when compared to wild type cells (Fig. 1B, 1C, 1D, 1E).

Consistent with our previous studies on rat pulmonary arterial myocytes (*14*), the response of mouse myocytes to NAADP was abolished by depletion of acidic Ca^{2+} stores with bafilomycin-A1 (Fig. 1F) and attenuated following depletion of sarcoplasmic reticulum (SR) Ca^{2+} stores by pre-incubation with the SR Ca^{2+} ATPase inhibitor thapsigargin (Fig. 1G), suggesting that lysosomal Ca^{2+} bursts are subsequently amplified by Ca^{2+}-induced Ca^{2+} release from SR stores. Nevertheless, the failure of NAADP to induce Ca^{2+} transients in myocytes from *Tpcn2* knockout mice was not due to the loss of releasable, acidic Ca^{2+} stores, because pronounced Ca^{2+} transients were evoked upon lysis of lysosomes by glycyl-L-phenylalanine-2-naphthylamide (GPN, (*15*); Fig. 1H, 1I) and upon depletion of acidic stores by application of the vacuolar proton pump (V-H^+-ATPase) inhibitor bafilomycin-A1 (Fig. 1J, 1K, 1L, 1M). Furthermore and consistent with previous studies (*16-19*), we found that two different voltage-gated Ca^{2+} channel antagonists, the dihydropyridine nifedipine and the phenylalkylamine verapamil, blocked NAADP-induced Ca^{2+} signals in pulmonary arterial myocytes (Fig. 2A, 2B) and in HEK293 cells stably over-expressing hTPC2 (Fig. 2C) to comparable extents (Fig. 2D). These results are consistent with verapamil blocking the Na^+ conductance carried by hTPC2 (*9*). From these data, we conclude that irrespective of the continued presence of releasable, acidic Ca^{2+} stores, TPC1, functional ryanodine receptors and I(1,4,5)P_3 receptors, TPC2 is required for the induction of global Ca^{2+} signals by NAADP, but by contrast is not necessary for Ca^{2+} signaling by PI(3,5)P_2, I(1,4,5)P_3 or cADPR, at least in the cell types studied here. Consistent with this view, double blind paired analysis showed that intracellular dialysis of NAADP induced Ca^{2+} transients in HEK293 cells that stably over-expressed EGFP-tagged hTPC2 but not in those expressing its inactive mutant (N653K) that does not support Na^+ conductance (Fig. S1A, S1B). As previously reported (*9*), we found by direct electrophysiological measurements of isolated lysosomes that hTPC2 conferred a PI(3,5)P_2-gated, NAADP-insensitive Na^+ conductance. However, in the presence of high luminal and "cytoplasmic" Ca^{2+} (60 mM pipette, 200 μM bath, which reproduces previously used conditions (*11*)), TPC2 supported an NAADP- and PI(3,5)P_2-sensitive Ca^{2+} conductance in our hands (Fig. S2A, S2B, S2C, S2E), consistent with previous reports on the capacity of TPC2 to support a small (*7*), NAADP-sensitive Ca^{2+} conductance (*11*).

Rapamycin induces Ca^{2+} signals through acidic stores in an mTOR- and TPC2-dependent manner

Extracellular application of rapamycin induced concentration-dependent Ca^{2+} signals in hTPC2 expressing HEK293 cells (Fig. 3A, 3B, 3C, 3D, 3E, 3H); by contrast rapamycin induced small Ca^{2+} transients in wild type HEK293 cells, which have low TPC2 abundance (*2*). Rapamycin triggered Ca^{2+} transients in hTPC2 expressing HEK293 cells at as low a concentration as 100 nmol/L (Fig. 3A). At the higher concentrations tested, rapamycin-evoked Ca^{2+} transients were multi-phasic, characterized by an initial large transient followed by Ca^{2+} oscillations that were variable in number and magnitude, and all were superimposed upon what appeared to be a slower, more uniform and prolonged Ca^{2+} signal (Fig. 3I). However, the concentration-response curve for rapamycin-induced Ca^{2+} signals was bell-shaped, peaking at 30 μmol/L and exhibiting progressive levels of "desensitization" between 100 and 300 μmol/L, at which concentration rapamycin-induced desensitization occurred without a prior Ca^{2+} signal being evoked (Fig. 3H). These results are consistent with our previous reports on the nature of the response of these cells (*20*) and the response of pulmonary arterial myocytes (*14*) to NAADP. Although rapamycin inhibits mTORC1 at low concentrations, we found that at the high concentration that gave the peak response in the Ca^{2+} assay (30 μmol/L), the drug decreased mTORC1 activity in HEK293 cells faster than at the lower concentrations (300 nmol/L), as indicated by S6K phosphorylation (Fig. S3A, S3B). Therefore, 30 μmol/L rapamycin was used in all subsequent experiments to insure robust and reproducible responses.

The response to 30 μmol/L rapamycin (Fig. 3I) was abolished by prior depletion of acidic Ca^{2+} stores with bafilomycin-A1 (Fig. 3J) and attenuated by pre-incubation of cells with thapsigargin (Fig. 3K). Thapsigargin blocked the fast oscillating Ca^{2+} transients but not the slow progressive rise in Ca^{2+} on which these were superimposed, suggesting that the Ca^{2+} oscillations likely result from Ca^{2+}-induced Ca^{2+} release from the endoplasmic reticulum triggered by prior Ca^{2+} release from acidic Ca^{2+} stores. Furthermore, all signals were abolished by pre-incubation of cells with nifedipine (Fig. 3L). In pulmonary arterial myocytes, rapamycin induced Ca^{2+} transients that were mostly biphasic, characterized by a single rapid, global Ca^{2+} transient which was once again superimposed on an underlying, slower transient (Fig. 3M). Occasionally the initial, fast Ca^{2+} transient was, as for HEK293 cells, followed by multiple smaller transients which were all superimposed on the slower underlying Ca^{2+} signal, but for pulmonary arterial myocytes such Ca^{2+} oscillations were not a common feature of the response to rapamycin. In pulmonary arterial myocytes, rapamycin-evoked Ca^{2+} transients were blocked by prior depletion of acidic Ca^{2+} stores with bafilomycin-A1 (Fig. 3N), attenuated by pre-incubation with thapsigargin (Fig. 3O) or ryanodine (Fig. 3O), and abolished by pre-incubation with nifedipine (Fig. 3P). These results were similar to those obtained in HEK293 cells stably

over-expressing hTPC2 and to that previously reported for NAADP-evoked Ca^{2+} signals in pulmonary arterial myocytes (*14*). Due to the more complex nature of rapamycin-induced Ca^{2+} signals, from this point forward we analyzed the responses for mTOR inhibition by measuring the "area under the curve" (AUC) which may provide a more accurate assessment of outcomes (Fig. 4A, 4B). Consistent with previous findings of others for TPC2 (*19*), rapamycin- and NAADP-induced Ca^{2+} transients were also blocked by tetrandrine (Fig. 4C, 4D), which has previously been shown to activate autophagy (*21*) and block TPC2 (*22*). Moreover, similar to rapamycin, the mTOR inhibitor torin-2 also evoked biphasic Ca^{2+} transients in HEK293 cells stably over-expressing hTPC2 and in pulmonary arterial myocytes (Fig. 4C, 4D). These Ca^{2+} transients exhibited characteristics similar to those induced by NAADP (Fig. S4A, S4B, S4C, S4D). Increases in cytoplasmic Ca^{2+} concentration were also induced by torin-1, but these were sustained and did not return to baseline during the course of these experiments (Fig. S5A, S5B, S5C).

Neither rapamycin nor torin-2 induced measurable Ca^{2+} transients in myocytes derived from *Tpcn2* knockout mice (Fig. 5A, 5B, 5C). Moreover, shRNA knockdown of mTOR in HEK293 cells that stably overexpressed hTPC2 attenuated Ca^{2+} transients induced by rapamycin and NAADP (Fig. 5D, 5G). These data suggest that rapamycin induces Ca^{2+} transients in a TPC2-dependent manner by inhibiting mTOR, and TPC2 may therefore be the point of convergence for the induction of Ca^{2+} signals by NAADP and mTOR inhibition. This notion was confirmed by cross-desensitization of signaling between mTOR inhibition and NAADP. NAADP-induced Ca^{2+} signals were abolished by pre-incubation with rapamycin or torin-2 in both pulmonary arterial smooth muscle cells (Fig. 6A, 6B, 6C, 6D) and in HEK293 cells that stably over-expressed hTPC2 (Fig. 6E, 6H). However, the effects of prior intracellular dialysis of high, desensitizing concentrations of NAADP on rapamycin-induced Ca^{2+} signals were more variable, but generally appeared to have little effect. In rat pulmonary arterial myocytes, following intracellular dialysis of NAADP, Ca^{2+} transients evoked by rapamycin were marginally attenuated only when assessed by AUC and these differences were not significant (Fig. 6C, 6D). Moreover, in hTPC2-HEK293 cells, prior intracellular dialysis of desensitizing concentrations of NAADP did not affect Ca^{2+} transients (Fig. 6G, 6H). This contrary outcome may be due to disparities with respect to the amount of time in which pulmonary arterial myocytes and hTPC2 expressing HEK293 cells could be held in the whole-cell configuration and the time-dependence of the process of desensitization by high concentrations of NAADP. Alternatively, NAADP may self-desensitize this macromolecular signaling complex at a point upstream of mTOR.

Rapamycin evokes bafilomycin-A1- and nifedipine-sensitive Ca^{2+} signals proximal to TPC2 in HEK293 cells

We next used HEK293 cells that stably over-expressed GCaMP5-hTPC2, in which the genetically encoded Ca^{2+} indicator GCaMP5 was fused to the cytoplasmic N-terminus of TPC2, allowing detection of Ca^{2+} signals arising near the lysosome-localized TPC2. Confocal imaging showed that GCaMP5-hTPC2 specifically labeled Lysotracker-red positive vesicles, which formed either static clusters of variable density or smaller motile units (Fig. 7A). Application of rapamycin induced slowly developing increases in fluorescence that arose and returned to baseline with a time course of 60-120s (Fig. 7B). These followed a similar time course to the slower, thapsigargin-insensitive signals recorded by way of Fura-2 fluorescence ratio (Fig. 3K). These findings suggest that the sampling interval (0.2 Hz) for confocal experiments did not provide the temporal resolution necessary to reveal those fast Ca^{2+} transients superimposed on the slower, thapsigargin-insensitive components of rapamycin-induced signals described above. Consistent with this view, these signals were blocked by prior depletion of acidic stores by bafilomycin-A1 and by pre-incubation with nifedipine, but were not affected by pre-incubation of cells with thapsigargin (Fig. 7C, 7D, 7E). Furthermore, nifedipine reduced basal fluctuations in GCaMP5-hTPC2 fluorescence relative to control, providing indirect support for the view that this L-type voltage-gated Ca^{2+} channel antagonist directly inhibits lysosomal Ca^{2+} efflux, whether through TPC2 or a distinct pathway governed by activation of TPC2.

DISCUSSION

Using fully differentiated, acutely isolated pulmonary arterial myocytes to examine the role of TPC2 in lysosomal Ca^{2+} signaling (*23-25*) in combination with HEK293 cell lines stably over-expressing human TPC2, we showed that TPC2 was required for global Ca^{2+} transients in response to intracellular dialysis of NAADP. Briefly, NAADP failed to induce global Ca^{2+} transients in pulmonary arterial myocytes from *Tpcn2* knockout mice although both lysosomes and the SR retained replete and releasable Ca^{2+} stores, mobilisation of the former being triggered by GPN and bafilomycin-A1, and the latter by intracellular dialysis of $I(1,4,5)P_3$ and cADPR. TPC1 (*2*), ryanodine receptors and $I(1,4,5)P_3$ receptors remain available in pulmonary arterial myocytes (*14, 20, 24-26*) from *Tpcn2* knockout mice, thereby demonstrating that TPC2 is required for the induction of global Ca^{2+} waves by NAADP in this cell type (*24, 25*).

These findings recapitulate our previous observations on HEK293 cells, which suggested that over-expression of hTPC2 is required to support NAADP-dependent global Ca^{2+} signals (*2, 20*), and that recombinant expression of ryanodine receptors is required for cADPR-induced Ca^{2+} transients (*20*). These findings are consistent with the observation that HEK293 cells primarily rely on $I(1,4,5)P_3$ receptors to mediate global Ca^{2+} signals, while exhibiting little or no endogenous functional expression of either TPCs (*2*) or ryanodine receptors (*27*). On the other hand, these findings argue against the proposal that $PI(3,5)P_2$-gated Ca^{2+} signals arise in a TPC2-dependent manner in these cells, regardless of whether TPC2 itself supports a Na^+-specific conductance (*9*) or both Ca^{2+} and Na^+ conductances (*11*). This view was strengthened by our studies on HEK293 cells and pulmonary arterial myocytes, in which we found that $PI(3,5)P_2$ not only evoked Ca^{2+} oscillations in HEK293 cells stably overexpressing hTPC2 and pulmonary arterial myocytes derived from wild type mice, but that $PI(3,5)P_2$ also did so in pulmonary arterial myocytes from *Tpcn2* null mice and in wild type HEK293 cells, in which endogenous expression of TPC2 is too low to support NAADP-dependent global Ca^{2+} signals (*2, 20*). These outcomes are therefore consistent with the retention of $PI(3,5)P_2$-gated cation currents in cells from *Tpcn1* and *Tpcn2* double knockout mice (*11*). Accordingly, others have shown that $PI(3,5)P_2$ can gate various channel families other than TPCs, including TRPML1 and ryanodine receptors (*28-30*). We cannot, however, rule out the possibility that $PI(3,5)P_2$ availability is required to support TPC2 activity.

We found that rapamycin and another mTOR inhibitor torin-2 also induced Ca^{2+} signals by mobilizing bafilomycin-A1-sensitive, acidic stores in a manner that was markedly attenuated by shRNA knockdown of

mTOR and abolished by *Tpcn2* deletion. These data suggest that mTOR inhibitors induce Ca^{2+} release from lysosomes through TPC2 in an mTOR-dependent manner rather than by directly binding to TPC2, although we cannot rule out the possibility that some mTOR inhibitors may also directly activate TPC2; torin-1 appeared to have a distinct mode of activating TPC2 (Fig. S5A, S5B, S5C, S5D). Moreover, using HEK293 cells stably over-expressing GCaMP5-hTPC2 we showed that rapamycin increased lysosomal Ca^{2+} flux proximal to hTPC2 itself. This finding is not inconsistent with the findings of others which suggest that mTOR is an endogenous inhibitor of $PI(3,5)P_2$-gated Na^+ currents carried by TPC2 (*10*). Although small when compared to their estimated Na^+ permeability, it appears that endogenous TPC2 may support a Ca^{2+} conductance sufficient to trigger global Ca^{2+} signals due to amplification of lysosomal Ca^{2+} bursts at lysosome-sarcoplasmic reticulum nanojunctions (*23-25*), as has been suggested by computer simulations (*23*) and electrophysiological investigations on the ion selectivity conferred by the filter sequence of the human TPC2 channel pore (*7*) and whole-endolysosomal recordings for human TPC2 carried out with Ca^{2+} as the major permeant ion by others (*7*)) and us (Fig. S2A, S2B, S2C, S2D). This notion is supported by our demonstration of cross-desensitisation between mTOR inhibitor and NAADP with respect to their capacity to evoke Ca^{2+} signals in both pulmonary arterial myocytes and in HEK293 cells stably over-expressing hTPC2. This observation is consistent with the indirect activation of TPC2 by NAADP through associated proteins (*31, 32*) and may confirm the primary physiological role of TPC2, in that mTOR-dependent Ca^{2+} mobilization may modulate the luminal pH of lysosomes (*33, 34*) and thus autophagic flux (*12, 35*).

We conclude that inactivation of mTOR is a major endogenous pathway for initiating lysosomal Ca^{2+} release in HEK293 cells stably overexpressing hTPC2 and in pulmonary arterial myocytes. Thus, the mTORC1-TPC2 complex may act as the endogenous gatekeeper of lysosomal Ca^{2+} flux, which may in turn impact autophagy termination and mTOR reactivation (*12*). Because mTORC1-dependent myocyte proliferation promotes the progression of pulmonary hypertension (*13*), for which current therapies are ineffective, TPC2 may be a potential therapeutic target in idiopathic pulmonary hypertension and pulmonary hypertension secondary to lysosomal dysfunction associated with Pompe and Gaucher diseases (*36, 37*). In this respect, our demonstration that nifedipine attenuates basal, NAADP- and rapamycin-evoked lysosomal Ca^{2+} release in a TPC2-dependent manner is notable, because this Ca^{2+} channel antagonist is used in the treatment of pulmonary hypertension (*38, 39*).

MATERIALS AND METHODS

Preparation of pulmonary arterial smooth muscle cells and HEK293 cell lines stably expressing human TPC2.

Experiments were performed in accordance with the United Kingdom Animals (Scientific Procedures) Act 1986.

Single arterial smooth muscle cells were isolated from second order branches (external diameter ~1mm) of the pulmonary artery. Briefly, the arteries were dissected from lungs of male wild type (C57/Bl6) and *Tpcn2* knockout(*2*) mice (28-33g), or Wistar rats (250-300g), and single cells acutely isolated from pulmonary arterial smooth muscle from mouse or rat as previously described(*24*), and placed in low Ca^{2+} solution of the following composition (in mmol / L): 135 NaCl, 5 KCl, 1 $MgCl_2$, 0.5 NaH_2PO_4, 0.5 KH_2PO, 15 $NaHCO_3$, 0.16 $CaCl_2$, 0.5 EDTA, 10 glucose, 10 taurine, and 10 Hepes, pH 7.4. For cell isolation, dissected arteries were transferred into fresh low Ca^{2+} solution containing (in mg / ml) 1 papain, 0.8 dithiothreitol and 0.7 bovine serum albumin and incubated for 10 min at 37ºC and gently triturated using a fire polished glass pipette in order to obtain dispersed pulmonary arterial smooth muscle cells (PASMCs). Acutely isolated PASMCs were then plated in a 35-mm cell-culture dish (Fluorodish - World Precision Instruments Inc.) and used within 24 hrs. The HEK293 cell line stably expressing human TPC2 was also developed and cultured as previously described *(2)*. Site-directed mutagenesis was performed to generate a TPC2 N653K mutant that lacked a Na^+ conductance, using the QuikChange Site-Directed Mutagenesis Kit (Stratagene). The mutation was confirmed by DNA sequencing.

Ca^{2+} imaging

Cells were incubated for 30 min with 5 μM Fura-2-AM in nominally Ca^{2+} free physiological salt solution (PSS) of the following composition (in mmol / L): 130 NaCl, 5.2 KCl, 1 $MgCl_2$, 10 glucose, 10 Hepes, pH 7.45, in an experimental chamber that was then placed on a Leica DMIRBE inverted microscope after washing with Ca^{2+} containing (1.7 mmol / L $CaCl_2$), Fura-2 free PSS for at least 30 min prior to experimentation. PSS was of the following composition (mmol / L): 130 NaCl, 5.2 KCl, 1 $MgCl_2$, 1.7 $CaCl_2$, 10 glucose, 10 Hepes, pH 7.45. Cytoplasmic Ca^{2+} concentration was reported by Fura-2 fluorescence ratio (F340 / F380 excitation; emission 510 nm). Emitted fluorescence was recorded at 22 °C with a sampling frequency of 0.5 Hz, using a Hamamatsu 4880 CCD camera and a Zeiss Fluar 40x, 1.3 n.a. oil immersion objective. Background subtraction was performed on-line. Analysis was completed using Openlab imaging

software (Perkin-Elmer, UK). NAADP (10 nmol / L) was applied intracellularly into single cells in the whole-cell configuration of the patch-clamp technique (voltage-clamp mode; holding potential = -40 mV). The pipette solution contained (in mmol / L): 140 KCl, 10 Hepes, 1 $MgCl_2$ and 5 µmol / L Fura-2 (free acid), pH 7.4, nominally Ca^{2+} free (~100 nmol / L). The seal resistance was ≥3 GΩ throughout each experiment. Series and pipette resistance was ≤10 MΩ and ≤3 MΩ, respectively, as measured by an Axopatch 200B amplifier (Axon Instruments).

Confocal microscopy

The GCaMP5 fluorescence ratio (expressed as F/F_0; F_0 = GCaMP5 fluorescence intensity at 0s; F_x = fluorescence intensity at time x for given region of interest) was recorded at 22 °C with a sampling frequency of 0.5 Hz, using A Nikon A1R+ confocal system and a Nikon Eclipse Ti inverted microscope with a Nikon Apo 40x λS DIC N2, 1.25 n.a. water immersion objective (Nikon Instruments Europe BV, Netherlands). Experiments were processed with ImageJ software (Rasband WS. ImageJ, U.S. National Institutes of Health, Bethesda, Maryland, USA, imagej.nih.gov/ij/, 1997—2012).

Analysis of mTOR activities in response to rapamycin treatment by immunoblotting

HEK293 cells were seeded in 6-well plates at 40~50% confluence and cultured overnight to reach ~70% confluence. Rapamycin was diluted to final concentrations of 0.3 µM and 30 µM in complete culture medium (DMEM supplemented with 10% fetal bovine serum) and warmed to 37°C before being added to the cells. At desired times (1-60 min) after the addition of rapamycin, the medium was aspirated and 200 µl of 1X SDS sampling buffer (50 mM Tris-HCl, 2% SDS, 10% glycerol, 1% β-mercaptoethanol, 12.5 mM EDTA and 0.02% bromophenol blue, pH 6.8) were immediately added to cause cell lysis. Cell lysates were then collected into 1.5 ml Eppendorf tubes and sonicated for 15 seconds before boiling at 99°C for 5 min. Lysates were resolved in 7.5% Tris-Glycine SDS-PAGE gel and analyzed using mouse-anti-phospho-S6K (Thr^{389}) (1:1000, Cell Signaling Technology Cat # 9206) and rabbit-anti-S6K (1:1000, Cell Signaling Technology Cat # 9202) primary antibodies. Dylight 800 goat-anti-mouse (1:5000, Invitrogen Cat # SA5-10176) and Dylight 680 goat-anti-rabbit (1:5000, Invitrogen Cat # 21109) secondary antibodies were used to reveal signals and blots were scanned with fluorescent immunoblot instruments and software by LI-COR Odyssey Software Images.

Whole-endolysosome patch clamp experiments

Endolysosomal patch clamp recordings were performed in isolated enlarged endolysosomes using a modified patch-clamp method (*9,11,40*). HEK293 cells stably expressing TPC2-EGFP were treated with 1 μM vacuolin-1 for 12-36 hrs. Electrophysiological recordings were performed using an EPC10 USB acquisition system (HEKA). Patchmaster software (HEKA) was used to record and analyze data. Recording solutions followed either that by Ruas *et al.* (*11*) or that by Wang *et al.* (*9*), which differ mainly in that the pipette solution was either Ca^{2+}-rich (Na^{+}-free) or Na^{+}-rich, respectively. The Ca^{2+}-rich pipette solution contained (in mM) 70 K-methanesulfonate (MSA), 60 Ca-MSA, 1 $MgCl_2$, 10 HEPES (pH adjusted with MSA to 4.6 and mannitol used to adjust osmolarity); the bath solution contained (in mM) 130 K-MSA, 0.2 mM Ca-MSA, 10 HEPES (pH adjusted with KOH to 7.2). The Na^{+}-rich pipette solution had (in mM) 145 NaCl, 5 KCl, 2 $CaCl_2$, 1 $MgCl_2$, 10 HEPES, 10 MES, 10 glucose (pH adjusted with NaOH to 4.6); the bath solution contained (in mM) 140 K-gluconate, 4 NaCl, 1 EGTA, 2 $MgCl_2$, 0.39 $CaCl_2$, 20 HEPES (pH adjusted with KOH to 7.2; free $[Ca^{2+}]$ = 100 nM). In brief, an isolated pipette was used to slice the cell membrane and release endolysosomes labeled with EGFP fluorescence. Only one enlarged endolysosome vacuole was recorded from each coverslip. Then a freshly polished recording pipette was used to form a gigaseal to the vacuole. ZAP pulses (fast pulses of -400 mV to -1,000 mV in 50 ms to 100 ms durations) were used to establish the whole-endolysosome configuration. Capacitance transients were compensated automatically. The holding potential was set at 70 mV and inside out recording mode was used for data acquisition, in which the inward currents were defined as currents flowing out of lysosomal lumen into the cytosol. Voltage ramps from -150 mV to +150 mV within 200 ms were applied every second. A 20 ms step to -150 mV and a 20 ms step to +150 mV were included at the beginning and end, respectively, of each ramp. Currents at -150 mV were used for further analysis.

Data presentation and statistical analysis

Data are presented as the mean ± SEM for *n* experiments. Comparisons between groups were by Kruskal Wallis test with Dunn's multiple comparison test, and non-parametric unpaired t-test. Probability values less than 0.05 were considered to be statistically significant.

Drugs and chemicals

Unless otherwise stated all compounds were from Sigma-Aldrich.

SUPPLEMENTARY MATERIALS

Fig. S1. Blind experiments on active and null hTPC2 constructs demonstrate robustness of intracellular dialysis technique.

Fig. S2. Na^+ and Ca^{2+} currents mediated by endolysosomal TPC2 in response to NAADP and $PI(3,5)P_2$.

Fig. S3. High and low concentrations of rapamycin suppress mTORC1 activities in HEK 293 cells at different rates.

Fig. S4. Torin-2 induces increases in intracellular Ca^{2+} in HEK 293 cells stably overexpressing hTPC2 and in rat pulmonary arterial myocytes.

Fig. S5. Torin-1 induces low-magnitude, sustained increases in intracellular Ca^{2+} in HEK 293 cells stably overexpressing hTPC2 and in rat pulmonary arterial myocytes.

REFERENCES AND NOTES

1. K. Ishibashi, M. Suzuki, M. Imai, Molecular cloning of a novel form (two-repeat) protein related to voltage-gated sodium and calcium channels. *Biochem Biophys Res Commun* **270**, 370-376 (2000).
2. P. J. Calcraft, M. Ruas, Z. Pan, X. Cheng, A. Arredouani, X. Hao, J. Tang, K. Rietdorf, L. Teboul, K. T. Chuang, P. Lin, R. Xiao, C. Wang, Y. Zhu, Y. Lin, C. N. Wyatt, J. Parrington, J. Ma, A. M. Evans, A. Galione, M. X. Zhu, NAADP mobilizes calcium from acidic organelles through two-pore channels. *Nature* **459**, 596-600 (2009).
3. P. J. Calcraft, O. Ogunbayo, J. Ma, A. Galione, G. C. Churchill, M. X. Zhu, A. M. Evans, Does nicotinic acid adenine dinucletoide phosphate elicit Ca^{2+} release via two-pore channel 2 in rat pulmonary arterial smooth muscle cells. *Proc. Physiol. Soc.* **13**, PC18 (2008).
4. M. Schieder, K. Rotzer, A. Bruggemann, M. Biel, C. A. Wahl-Schott, Characterization of two-pore channel 2 (TPCN2)-mediated Ca^{2+} currents in isolated lysosomes. *J Biol Chem* **285**, 21219-21222 (2010).
5. S. J. Pitt, T. M. Funnell, M. Sitsapesan, E. Venturi, K. Rietdorf, M. Ruas, A. Ganesan, R. Gosain, G. C. Churchill, M. X. Zhu, J. Parrington, A. Galione, R. Sitsapesan, TPC2 is a novel NAADP-sensitive Ca^{2+} release channel, operating as a dual sensor of luminal pH and Ca^{2+}. *J Biol Chem* **285**, 35039-35046 (2010).
6. V. Rybalchenko, M. Ahuja, J. Coblentz, D. Churamani, S. Patel, K. Kiselyov, S. Muallem, Membrane potential regulates nicotinic acid adenine dinucleotide phosphate (NAADP) dependence of the pH- and Ca^{2+}-sensitive organellar two-pore channel TPC1. *J Biol Chem* **287**, 20407-20416 (2012).
7. J. Guo, W. Zeng, Y. Jiang, Tuning the ion selectivity of two-pore channels. *Proc Natl Acad Sci U S A* **114**, 1009-1014 (2017).
8. M. X. Zhu, J. Ma, J. Parrington, P. J. Calcraft, A. Galione, A. M. Evans, Calcium signaling via two-pore channels: local or global, that is the question. *Am J Physiol Cell Physiol* **298**, C430-441 (2010).
9. X. Wang, X. Zhang, X. P. Dong, M. Samie, X. Li, X. Cheng, A. Goschka, D. Shen, Y. Zhou, J. Harlow, M. X. Zhu, D. E. Clapham, D. Ren, H. Xu, TPC proteins are phosphoinositide- activated sodium-selective ion channels in endosomes and lysosomes. *Cell* **151**, 372-383 (2012).
10. C. Cang, Y. Zhou, B. Navarro, Y. J. Seo, K. Aranda, L. Shi, S. Battaglia-Hsu, I. Nissim, D. E. Clapham, D. Ren, mTOR regulates lysosomal ATP-sensitive two-pore Na^+ channels to adapt to metabolic state. *Cell* **152**, 778-790 (2013).
11. M. Ruas, L. C. Davis, C. C. Chen, A. J. Morgan, K. T. Chuang, T. F. Walseth, C. Grimm, C. Garnham, T. Powell, N. Platt, F. M. Platt, M. Biel, C. Wahl-Schott, J. Parrington, A. Galione, Expression of Ca^{2+}-permeable two-pore channels rescues NAADP signalling in TPC-deficient cells. *EMBO J* **34**, 1743-1758 (2015).

12. P. H. Lin, P. Duann, S. Komazaki, K. H. Park, H. Li, M. Sun, M. Sermersheim, K. Gumpper, J. Parrington, A. Galione, A. M. Evans, M. X. Zhu, J. Ma, Lysosomal two-pore channel subtype 2 (TPC2) regulates skeletal muscle autophagic signaling. *J Biol Chem* **290**, 3377-3389 (2015).
13. D. A. Goncharov, T. V. Kudryashova, H. Ziai, K. Ihida-Stansbury, H. DeLisser, V. P. Krymskaya, R. M. Tuder, S. M. Kawut, E. A. Goncharova, Mammalian target of rapamycin complex 2 (mTORC2) coordinates pulmonary artery smooth muscle cell metabolism, proliferation, and survival in pulmonary arterial hypertension. *Circulation* **129**, 864-874 (2014)
14. F. X. Boittin, A. Galione, A. M. Evans, Nicotinic acid adenine dinucleotide phosphate mediates Ca2+ signals and contraction in arterial smooth muscle via a two-pool mechanism. *Circ Res* **91**, 1168-1175 (2002).
15. T. O. Berg, E. Stromhaug, T. Lovdal, O. Seglen, T. Berg, Use of glycyl-L-phenylalanine 2-naphthylamide, a lysosome-disrupting cathepsin C substrate, to distinguish between lysosomes and prelysosomal endocytic vacuoles. *Biochem J* **300**, 229-236 (1994).
16. A. N. Yusufi, J. Cheng, M. A. Thompson, J. C. Burnett, J. P. Grande, Differential mechanisms of Ca^{2+} release from vascular smooth muscle cell microsomes. *Exp Biol Med* **227**, 36-44 (2002).
17. A. N. Yusufi, J. Cheng, M. A. Thompson, E. N. Chini, J. P. Grande, Nicotinic acid-adenine dinucleotide phosphate (NAADP) elicits specific microsomal Ca^{2+} release from mammalian cells. *Biochem J* **353**, 531-536 (2001).
18. O. A. Ogunbayo, E. O. Agbani, J. Ma, M. X. Zhu, A. M. Evans, Voltage-gated calcium channel antagonists block Nicotinic acid adenine dinucleotide phosphate-induced calcium signals via Two Pore Segment Channel subtype 2. *Proc Physiol Soc* **25**, PC38 (2011).
19. X. Zong, M. Schieder, H. Cuny, S. Fenske, C. Gruner, K. Rotzer, O. Griesbeck, H. Harz, M. Biel, C. Wahl-Schott, The two-pore channel TPCN2 mediates NAADP-dependent Ca^{2+}-release from lysosomal stores. *Pflugers Arch*, (2009).
20. O. A. Ogunbayo, Y. Zhu, D. Rossi, V. Sorrentino, J. Ma, M. X. Zhu, A. M. Evans, Cyclic adenosine diphosphate ribose activates ryanodine receptors, whereas NAADP activates two-pore domain channels. *J Biol Chem* **286**, 9136-9140 (2011).
21. V. K. W. Wong, W. Zeng, J. Chen, X. J. Yao, E. L. H. Leung, Q. Q. Wang, P. Chiu, B. C. B. Ko, B. Y. K. Law, Tetrandrine, an Activator of Autophagy, Induces Autophagic Cell Death via PKC-alpha Inhibition and mTOR-Dependent Mechanisms. *Front Pharmacol* **8**, 351 (2017) .
22. Y. Sakurai, A. A. Kolokoltsov, C. C. Chen, M. W. Tidwell, W. E. Bauta, N. Klugbauer, C. Grimm, C. Wahl-Schott, M. Biel, R. A. Davey, Ebola virus. Two-pore channels control Ebola virus host cell entry and are drug targets for disease treatment. *Science* **347**, 995-998 (2015).
23. N. Fameli, O. A. Ogunbayo, C. van Breemen, A. M. Evans, Cytoplasmic nanojunctions between lysosomes and sarcoplasmic reticulum are required for specific calcium signaling. *F1000Res* **3**, 93 (2014).
24. N. P. Kinnear, F. X. Boittin, J. M. Thomas, A. Galione, A. M. Evans, Lysosome-sarcoplasmic reticulum junctions. A trigger zone for calcium signaling by nicotinic acid adenine dinucleotide phosphate and endothelin-1. *J Biol Chem* **279**, 54319-54326 (2004).
25. N. P. Kinnear, C. N. Wyatt, J. H. Clark, P. J. Calcraft, S. Fleischer, L. H. Jeyakumar, G. F. Nixon, A. M. Evans, Lysosomes co-localize with ryanodine receptor subtype 3 to form a trigger zone for calcium signalling by NAADP in rat pulmonary arterial smooth muscle. *Cell Calcium* **44**, 190-201 (2008).
26. F. Zhang, G. Zhang, A. Y. Zhang, M. J. Koeberl, E. Wallander, P. L. Li, Production of NAADP and its role in Ca^{2+} mobilization associated with lysosomes in coronary arterial myocytes. *Am J Physiol Heart Circ Physiol* **291**, H274-282 (2006).
27. D. Rossi, I. Simeoni, M. Micheli, M. Bootman, P. Lipp, P. D. Allen, V. Sorrentino, RyR1 and RyR3 isoforms provide distinct intracellular Ca2+ signals in HEK 293 cells. *J Cell Sci* **115**, 2497-2504 (2002).
28. X. P. Dong, X. Cheng, E. Mills, M. Delling, F. Wang, T. Kurz, H. Xu, The type IV mucolipidosis-associated protein TRPML1 is an endolysosomal iron release channel. *Nature* **455**, 992-996 (2008).
29. C. D. Touchberry, I. K. Bales, J. K. Stone, T. J. Rohrberg, N. K. Parelkar, T. Nguyen, O. Fuentes, X. Liu, C. K. Qu, J. J. Andresen, H. H. Valdivia, M. Brotto, M. J. Wacker, Phosphatidylinositol 3,5-bisphosphate (PI(3,5)P2) potentiates cardiac contractility via activation of the ryanodine receptor. *J Biol Chem* **285**, 40312-40321 (2010).

30. X. Feng, J. Xiong, Y. Lu, X. Xia, M. X. Zhu, Differential mechanisms of action of the mucolipin synthetic agonist, ML-SA1, on insect TRPML and mammalian TRPML1. *Cell Calcium* **56**, 446-456 (2014).
31. M. Ruas, K. Rietdorf, A. Arredouani, L. C. Davis, E. Lloyd-Evans, H. Koegel, T. M. Funnell, A. J. Morgan, J. A. Ward, K. Watanabe, X. Cheng, G. C. Churchill, M. X. Zhu, F. M. Platt, G. M. Wessel, J. Parrington, A. Galione, Purified TPC Isoforms Form NAADP Receptors with Distinct Roles for Ca^{2+} Signaling and Endolysosomal Trafficking. *Curr Biol* **20**, 703-709 (2010).
32. Y. Lin-Moshier, T. F. Walseth, D. Churamani, S. M. Davidson, J. T. Slama, R. Hooper, E. Brailoiu, S. Patel, J. S. Marchant, Photoaffinity labeling of nicotinic acid adenine dinucleotide phosphate (NAADP) targets in mammalian cells. *J Biol Chem* **287**, 2296-2307 (2012).
33. A. J. Morgan, L. C. Davis, S. K. Wagner, A. M. Lewis, J. Parrington, G. C. Churchill, A. Galione, Bidirectional Ca^{2+} signaling occurs between the endoplasmic reticulum and acidic organelles. *J Cell Biol* **200**, 789-805 (2013).
34. A. J. Morgan, A. Galione, NAADP induces pH changes in the lumen of acidic Ca^{2+} stores. *Biochem J* **402**, 301-310 (2007).
35. V. Garcia-Rua, S. Feijoo-Bandin, D. Rodriguez-Penas, A. Mosquera-Leal, E. Abu-Assi, A. Beiras, L. Maria Seoane, P. Lear, J. Parrington, M. Portoles, E. Rosello-Lleti, M. Rivera, O. Gualillo, V. Parra, J. A. Hill, B. Rothermel, J. R. Gonzalez-Juanatey, F. Lago, Endolysosomal two-pore channels regulate autophagy in cardiomyocytes. *J Physiol* **594**, 3061-3077 (2016).
36. S. Noori, R. Acherman, B. Siassi, C. Luna, M. Ebrahimi, Z. Pavlova, R. Ramanathan, A rare presentation of Pompe disease with massive hypertrophic cardiomyopathy at birth. *J Perinat Med* **30**, 517-521 (2002).
37. M. Jmoudiak, A. H. Futerman, Gaucher disease: pathological mechanisms and modern management. *Br J Haematol* **129**, 178-188 (2005).
38. A. M. Antezana, G. Antezana, O. Aparicio, I. Noriega, F. L. Velarde, J. P. Richalet, Pulmonary hypertension in high-altitude chronic hypoxia: response to nifedipine. *Eur Respir J* **12**, 1181-1185 (1998).
39. S. Rich, E. Kaufmann, P. S. Levy, The effect of high doses of calcium-channel blockers on survival in primary pulmonary hypertension. *N Engl J Med* **327**, 76-81 (1992).
40. C. C. Chen, C. Cang, S. Fenske, E. Butz, Y. K. Chao, M. Biel, D. Ren, C. Wahl-Schott, C. Grimm, Patch-clamp technique to characterize ion channels in enlarged individual endolysosomes. *Nat Protoc* **12**, 1639-1658 (2017).

Funding: This work was primarily funded by a British Heart Foundation Programme Grant (29885, to AME), and by NIH RO1 grants (GM 092759 to MXZ and AR 070752 to JM). JD also received support from the China Scholarship Council (201508060127). **Author contributions:** OAO and AME carried out calcium imaging of pulmonary arterial myocytes and HEK293 cells. OAO, JD and AME carried out confocal microscopy. OAO, JX and MXZ carried out shRNA knockdown of mTOR. JX generated the mutant constructs and performed immunoblotting. QW and XF carried out whole-endolysosomal recordings. JX and MXZ developed cell lines expressing human TPC2 and TPC2-GCaMP5. AME, MXZ and JM designed experiments. AME wrote and all authors commented on the manuscript. **Acknowledgements:** We would like to thank Dr Paul Skehel for his kind help and advice**. Competing Interests:** The authors declare that they have no competing interests. **Data and materials availability:** All data needed to evaluate the conclusions in the paper are present in the paper or the Supplementary Materials. Stable cell lines described in this paper will be distributed to qualified researchers in academic institutions, using an unmodified version of the Material Transfer Agreement (MTA) approved by University of Texas Health Science Center at Houston.

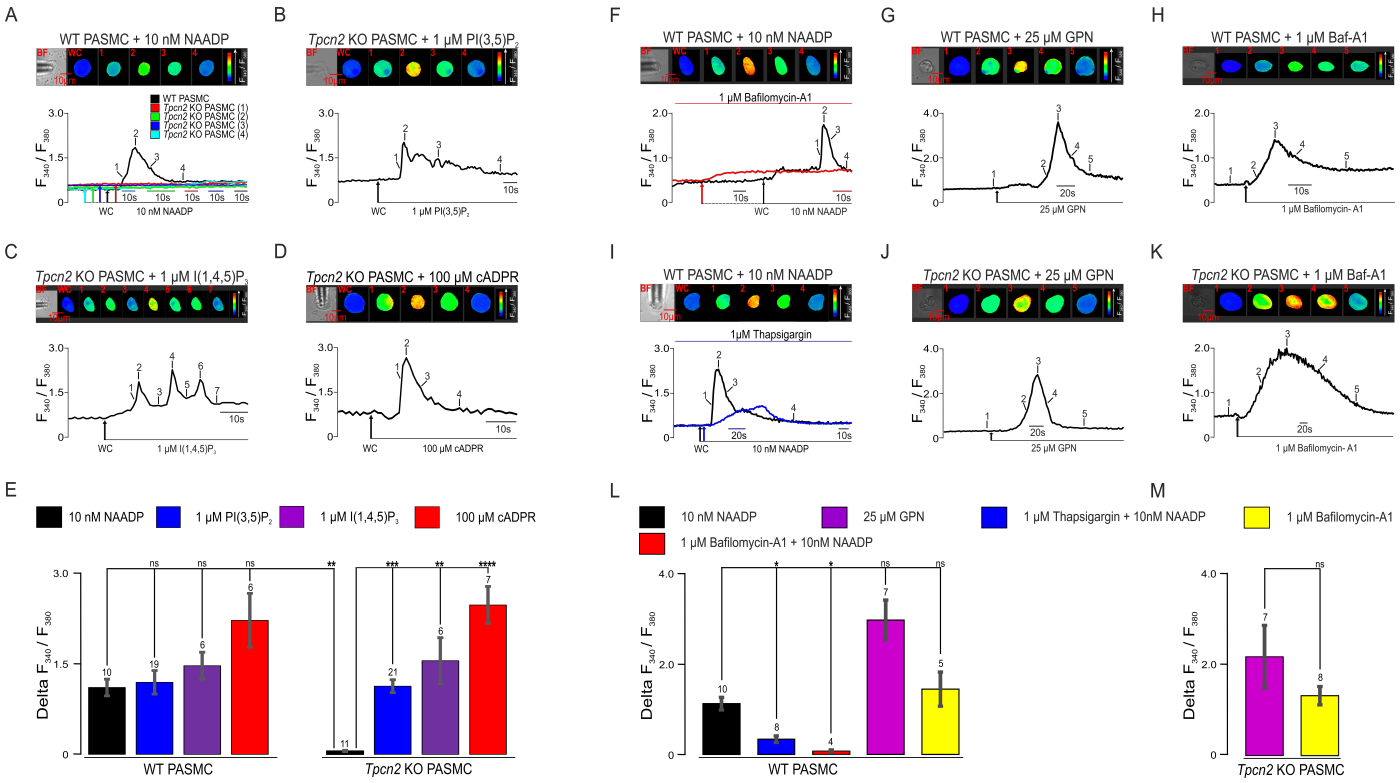

Fig. 1. Deletion of TPC2 in pulmonary arterial myocytes blocks Ca^{2+} transients evoked by NAADP but not those triggered by $PI(3,5)P_2$, $I(1,4,5)P_3$ or cADPR A, Upper panels show a bright field image of an acutely isolated mouse pulmonary arterial myocyte (PASMC), and a series of pseudo-colour images of the Fura-2 fluorescence ratio (F340/F380) recorded in the same cell during intracellular dialysis from a patch pipette of 10 nmol/L NAADP. Lower panel, corresponding record (black) of F340/F380 ratio against time; the time points at which pseudo-colour images were acquired are indicated by the numbered lines. WC indicates the beginning of intracellular dialysis upon entering the whole-cell configuration. The red, blue, cyan and green records show the effect of NAADP in myocytes from *Tpcn2* knockout mice. B-D, As in A but showing responses of myocytes from *Tpcn2* knockout mice to intracellular dialysis of $PI(3,5)P_2$ (B), $I(1,4,5)P_3$ (C) or cADPR (D). E, Bar chart shows the mean ± SEM for each stimulus across all cells studied (number of cells (n) indicated above bars). ns, not significant; $^{**}P < 0.01$; $^{***}P < 0.001$; $^{****}P < 0.0001$. F, Upper panel shows a bright field image of a PASMC acutely isolated from a wild type (WT) mouse, and a series of pseudo-colour images of the Fura-2 fluorescence ratio (F340 / F380) recorded in the same cell during intracellular dialysis from a patch pipette of 10 nmol / L NAADP. Lower panel, corresponding record (black) of F340 / F380 ratio against time; the time points at which pseudo-colour images were acquired are indicated by the numbered lines. WC indicates the beginning of intracellular dialysis upon entering the whole-cell configuration. Red record shows the effect of NAADP after pre-incubation (≥50 min) of a myocyte with 1 μmol / L bafilomycin-A1 (Baf-A1). G, as in F but with a blue record that shows the effect of NAADP in a different cell after pre-incubation with the SR Ca^{2+} ATPase inhibitor thapsigargin (1 μmol / L; ≥ 40 minutes). H, Shows the response of a WT mouse PASMC to extracellular application of 25 μmol / L GPN. I, as in H but showing the response of a myocyte from a *Tpcn2* knockout (KO) mouse. J and K, as in H and I but showing responses to 1 μmol / L bafilomycin-A1. L and M, Bar charts show the mean ± SEM (number of cells (n) indicated above bars) for the experiments shown in F, G, H and J for wild type (L) and I and K for *Tpcn2* KO mice (M). $^{*}P < 0.05$.

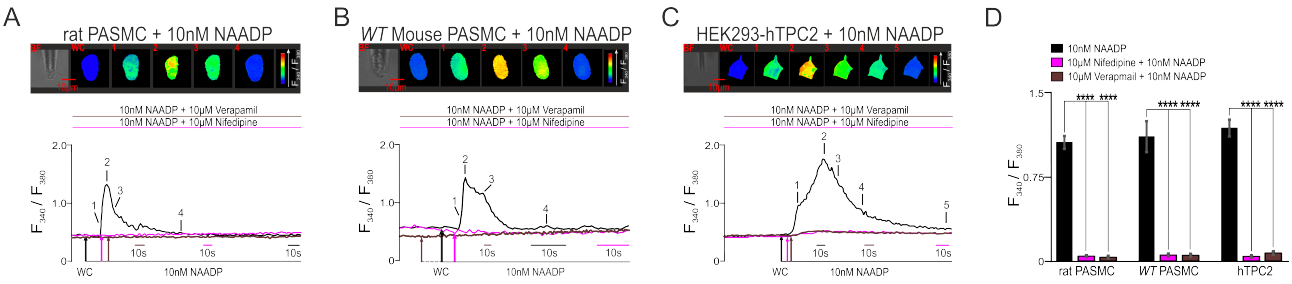

Fig. 2 Nifedipine and verapamil block NAADP-evoked Ca^{2+} transients A, Upper panels show a bright field image of an acutely isolated rat pulmonary arterial myocyte (PASMC), and a series of pseudo-colour images of the Fura-2 fluorescence ratio (F340 / F380) recorded in the same cell during intracellular dialysis from a patch pipette of 10 nmol / L NAADP. Lower panel, corresponding record (black) of F340 / F380 ratio against time; the time points at which pseudo-colour images were acquired are indicated by the numbered lines. WC indicates the beginning of intracellular dialysis upon entering the whole-cell configuration. The magenta and brown records show the effect of NAADP in myocytes pre-incubated with 10 μmol / L nifedipine and 10 μmol / L verapamil, respectively. B, as in A but for an acutely isolated wild type (WT) mouse PASMC. C, as in A but for a HEK293 cell stably over-expressing hTPC2. D, Bar chart shows the mean ± SEM for each stimulus across all cells studied (number of cells (n) indicated above bars). $*P < 0.05$, $**P < 0.01$, $***P < 0.001$.

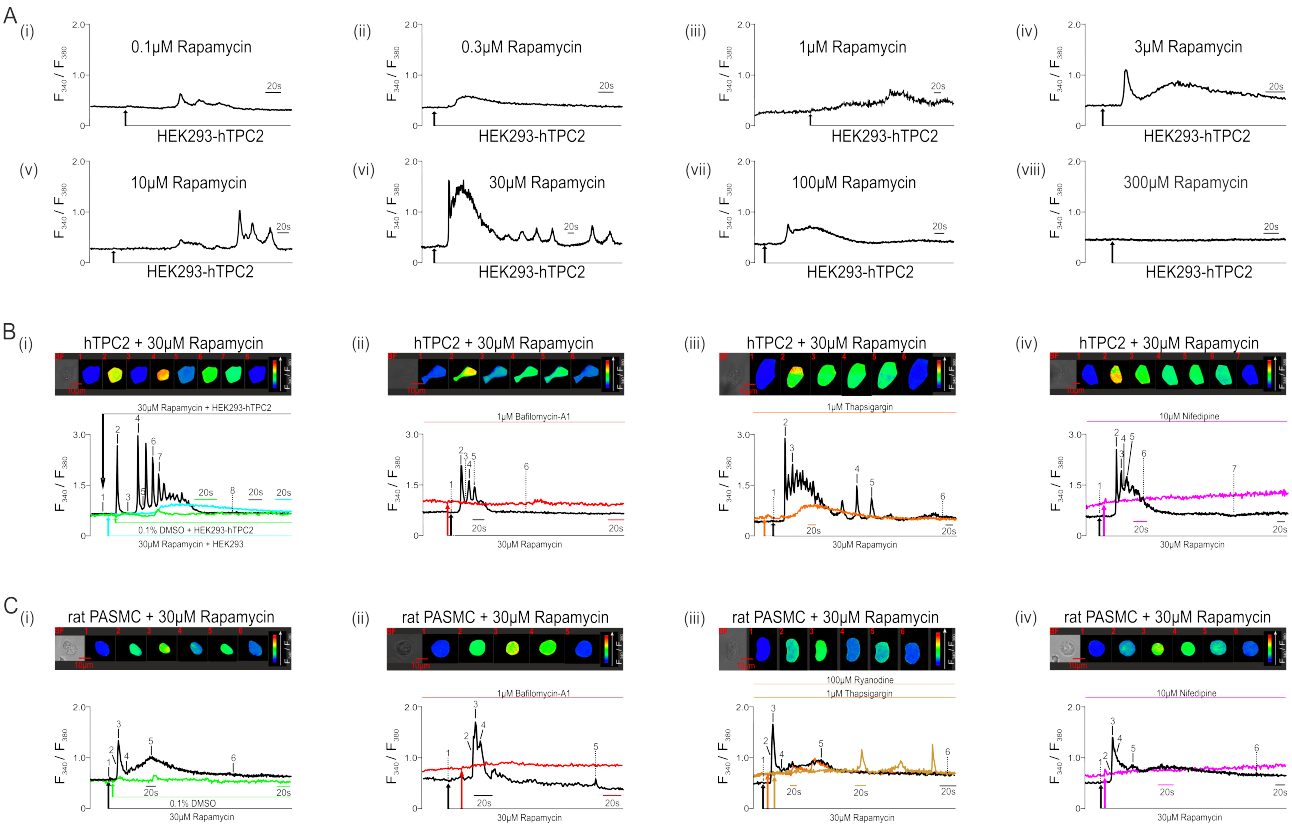

Fig. 3 Rapamycin induces Ca^{2+} transients in pulmonary arterial myocytes and hTPC2 expressing HEK293 cells that are blocked by bafilomycin A1 and nifedipine A to H, Example records (black) showing the concentration-response relationship as changes in Fura-2 fluorescence ratio (F340 / F380) against time during extracellular application of indicated concentrations of rapamycin (0.1-300 μmol / L) onto different HEK293 cells that stably expressed human TPC2. I, Upper panel shows a bright field image of a HEK293 cell stably over-expressing hTPC2, and a series of pseudo-colour images of F340/F380 recorded in the same cell during extracellular application of 30 μmol / L rapamycin. Lower panel, corresponding record (black) of F340 / F380 ratio against time; the time points at which pseudo-colour images were acquired are indicated by the numbered lines. Green record shows the effect of DMSO (vehicle control) in a different cell, and cyan record shows the effect of rapamycin on a wild type HEK293 cell. J, as in I but with a red record showing the effect of rapamycin after pre-incubation (≥50 min) of an hTPC2 expressing HEK293 cell with 1 μmol / L bafilomycin A1. K, as in I but with an orange record showing the effect of rapamycin after pre-incubation (≥50 min) of a cell with 1 μmol / L thapsigargin. L, as in I but with a magenta record showing the effect of rapamycin after pre-incubation (≥50 min) of a cell with 10 μmol / L nifedipine. M to P, as in I to L but for acutely isolated rat pulmonary arterial myocytes, except that O shows an additional record in gold of the effect of rapamycin after pre-incubation (≥50 min) of a myocyte with 10 μmol/L ryanodine.

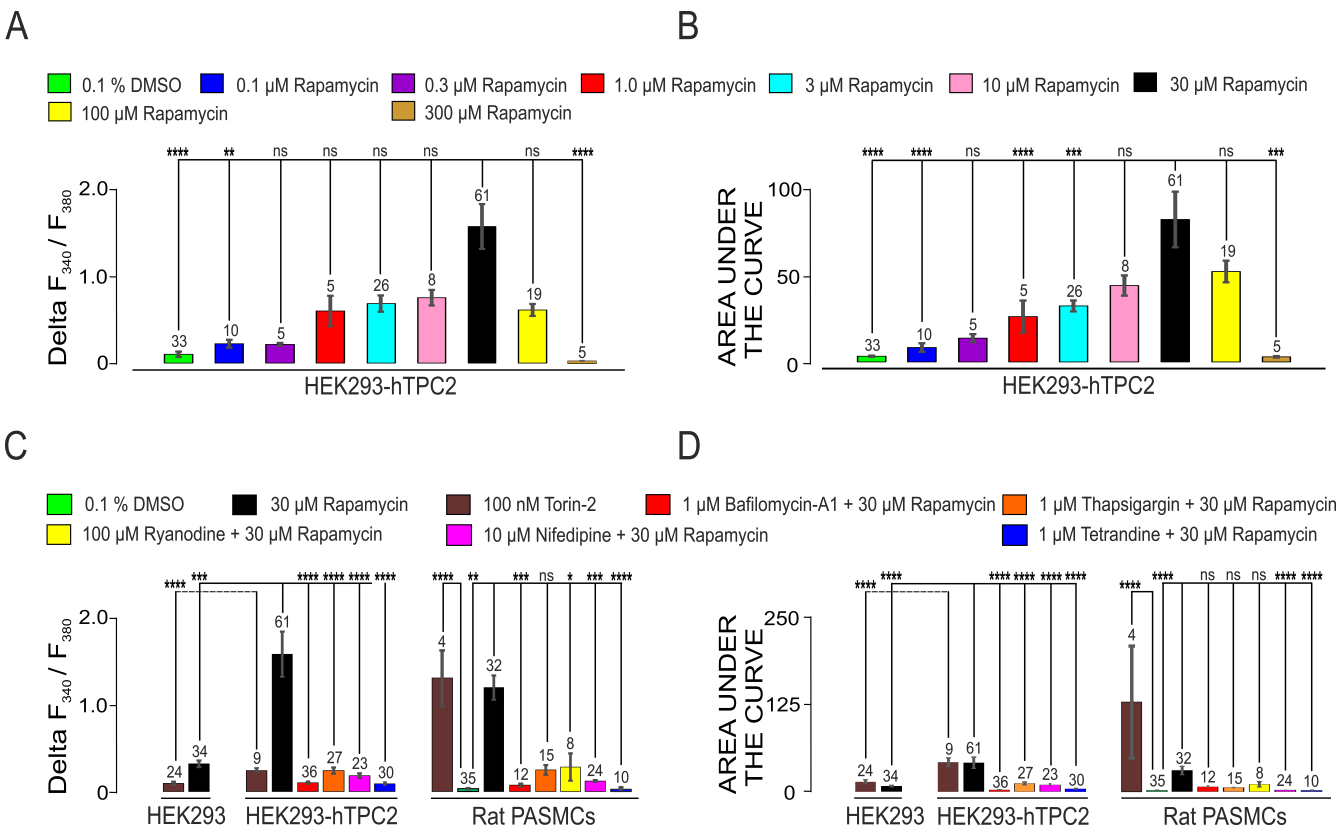

Fig. 4. Comparison of the effects of rapamycin and torin-2 in pulmonary arterial smooth muscle cells acutely isolated from rats or mice, wild type HEK293 cells and HEK293 cells stably over-expressing hTPC2. A, Bar chart showing the concentration-response relationship (mean ± SEM) for the peak change in Fura-2 fluorescence ratio (Delta F340 / F380) during extracellular application of rapamycin onto HEK293 cells that stably expressed hTPC2. B, as in A but for area under the curve. C**,** Bar chart compares the mean ± SEM for the peak change in Fura-2 fluorescence ratio during extracellular application of rapamycin onto wild type HEK293 cells, HEK293 cells that stably expressed hTPC2 and pulmonary arterial myocytes under all conditions studied (see key). D, as in C but for area under the curve (number of cells (n) indicated above bars). *$P < 0.05$, **$P < 0.01$, ***$P < 0.001$, ****$P < 0.0001$.

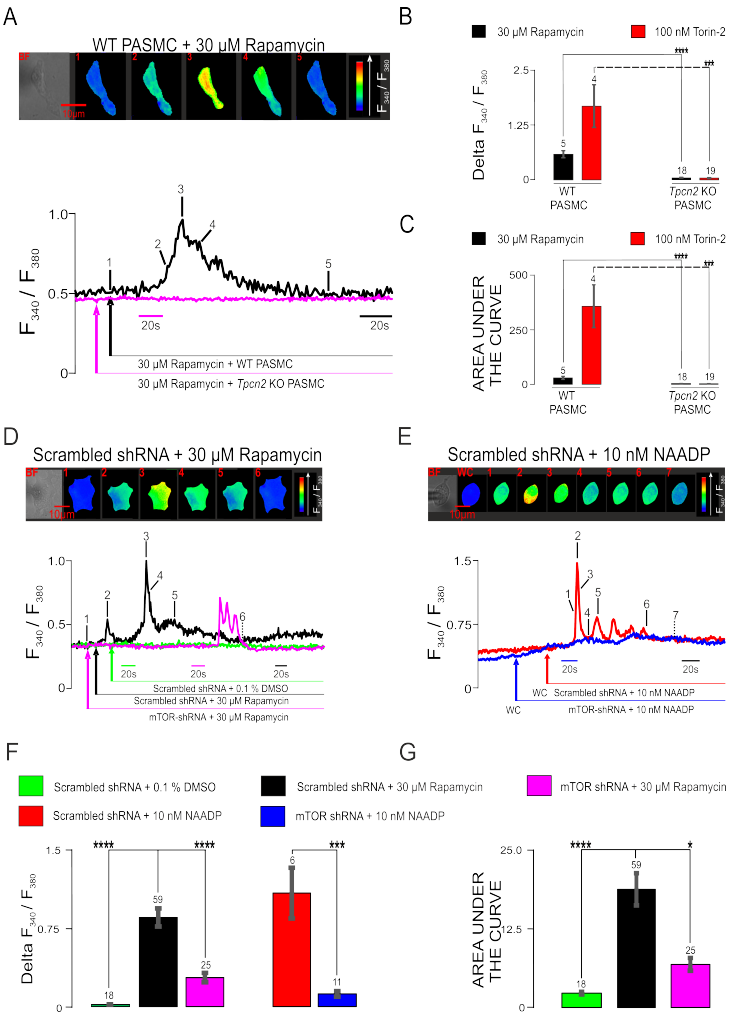

Fig. 5 Ca^{2+} transients induced by mTOR inhibitors in pulmonary arterial myocytes are blocked by deletion of TPC2 and by shRNA knockdown of mTOR. A, Upper panel shows a bright field image of a wild type (WT) mouse PASMC, and a series of pseudo-colour images of the Fura-2 fluorescence ratio (F340 / F380) recorded in the same cell during extracellular application of 30 μmol / L rapamycin. Lower panel, corresponding record (black) of F340/F380 ratio against time; the time points at which pseudo-colour images were acquired are indicated by the numbered lines. Pink record shows the response to 30 μmol / L rapamycin of a myocyte isolated from a *Tpcn2* knockout (*Tpcn*2 KO) mouse. B and C, bar charts show the mean ± SEM (number of cells (n) indicated above bars) for the peak change in F340 / F380 during the 1st transient recorded (B) and the area under the curve during the response of each cell to rapamycin and torin-2 (C). ***$P < 0.001$; ****$P < 0.0001$. D, Upper panel shows a bright field image of a HEK293 cell overexpressing hTPC2 48 hrs following transfection of scrambled shRNA, and a series of pseudo-colour images of the Fura-2 fluorescence ratio (F340/F380) recorded in the same cell during extracellular application of 30 μmol / L rapamycin. Lower panel, corresponding record (black) of F340 / F380 ratio against time; the time points at which pseudo-colour images were acquired are indicated by the numbered lines. Green and pink records showthe response to DMSO and 30 μmol / L rapamycin, respectively, of two different hTPC2 expressing HEK293 cells that were transfected with shRNA against mTOR. E, as in D but for different cells during intracellular dialysis with 10 nmol / L NAADP, as performed in Fig. 1; red record for a cell 48 hrs following transfection of scrambled shRNA and blue record for a cell transfected with shRNA against mTOR. F and G, bar chart shows the mean ± SEM (number of cells (n) indicated above bars) for the experiments shown in D and E, for the peak change in F340 / F380 ratio induced by NAADP and the peak change attained during the 1st transient recorded after rapamycin (C), and the area under the curve during the response to rapamycin (D). *$P < 0.05$, ***$P < 0.001$, ****$P < 0.0001$.

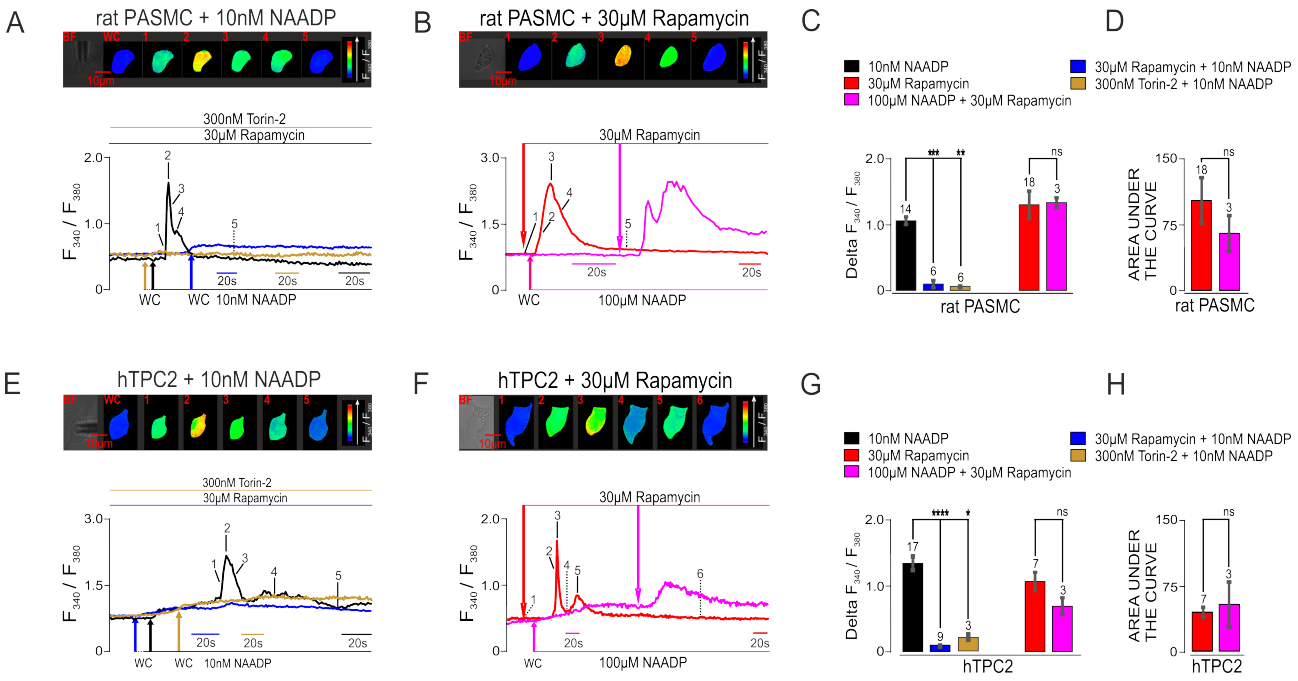

Fig. 6 Ca^{2+} transients evoked by mTOR inhibition and NAADP exhibit cross-desensitisation in pulmonary arterial myocytes and hTPC2 expressing HEK293 cells. A, Upper panel shows a bright field image of a rat PASMC, and a series of pseudo-colour images of the Fura-2 fluorescence ratio (F340 / F380) recorded in the same cell during intracellular dialysis of 10 nmol / L NAADP. Lower panel, corresponding record (black) of F340/F380 ratio against time; the time points at which pseudo-colour images were acquired are indicated by the numbered lines. WC indicates the beginning of intracellular dialysis upon entering the whole-cell configuration. Blue and brown records show, respectively, the response to 10 nmol/L NAADP of myocytes pre-incubated (30 min) with 30 μmol / L rapamycin or 300 nmol / L torin-2. B, as in A but for rapamycin in the absence of (red) and 2 min after intracellular dialysis of 100 μmol / L NAADP (pink). C and D, bar charts show the mean ± SEM for the experiments shown in A and B, for the peak change induced by 10 nmol / L NAADP and the peak change attained during the 1st transient recorded after 30 μmol / L rapamycin (C), and the area under the curve during the response to rapamycin (D). E-H, as in A-D but for HEK293 cells stably overexpressing hTPC2. Number of cells (n) indicated above bars. $*P<0.05$, $**P<0.01$, $***P<0.001$,$****P<0.0001$.

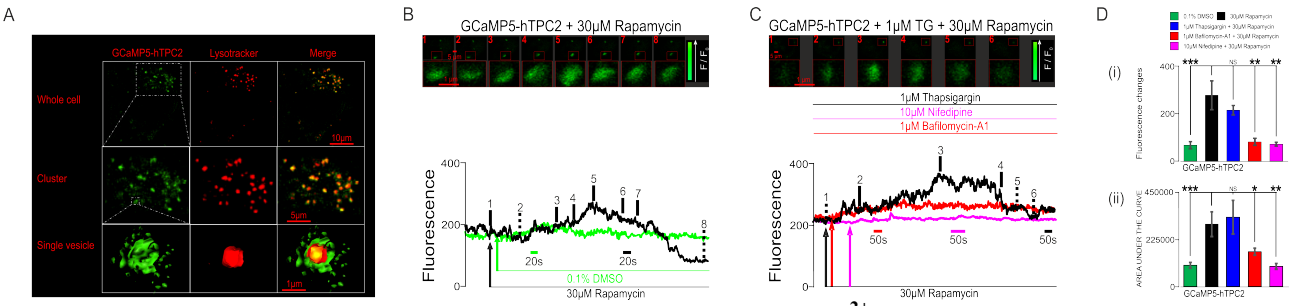

Fig. 7. Rapamycin induces bafilomycin and nifedipine-sensitive Ca^{2+} signals proximal to lysosomes in HEK293 cells that stably over-express GCaMP5-TPC2. A, Deconvolved confocal images show a 3D reconstruction, from left to right, of a single HEK293 cell stably expressing GCaMP5-hTPC2 (green), the distribution of Lysotracker-red (red) labeling within the same cell and a merged image depicting regions of colocalisation (yellow). B, Upper panels show confocal images of a HEK293 cell overexpressing GCaMP5-hTPC2 (Green) during extracellular application of 30 μmol / L rapamycin. Lower panel, corresponding record (black) of F/F_0 ratio against time; the time points at which confocal images were acquired are indicated by the numbered lines. Green record shows the effect of DMSO (vehicle control) in a different cell. C, as in B but showing the response of different cells to 30 μmol / L rapamycin after pre-incubation with 1 μmol / L thapsigargin (black), 1 μmol / L bafilomycin A1 (red) and 10 μmol / L nifedipine (pink). D and E, Bar charts show the mean ± SEM for the peak change in F/F_0 (D) and the area under the curve during the response to rapamycin (E). Number of cells (n) indicated above bars. $*P < 0.05$, $**P < 0.01$.